Published in: Cancer Research (2005), vol.65, iss.6, pp.2441-8
Status: Postprint (Author's version)

Mimicry of a Cellular Low Energy Status Blocks Tumor Cell Anabolism and Suppresses the Malignant Phenotype

Johannes V. Swinnen,[1] Annelies Beckers,[1] Koen Brusselmans,[1] Sophie Organe,[1] Joanna Segers,[1] Leen Timmermans,[1] Frank Vanderhoydonc,[1] Ludo Deboel,[1] Rita Derua,[2] Etienne Waelkens,[2] Ellen De Schrijver,[1] Tine Van de Sande,[1] Agnès Noël,[3] Fabienne Foufelle,[4] and Guido Verhoeven[1]

[1]Laboratory for Experimental Medicine and Endocrinology and [2]Division of Biochemistry, University of Leuven, Leuven, Belgium; [3]Laboratory of Tumor and Developmental Biology, University of Liege, Tour de Pathologie (B23), Sart-Tilman, Liege, Belgium; and [4]Institut National de la Santé et de la Recherche Médicale, Centre de Recherches Biomédicales des Cordeliers, Université Paris 6, Paris, France

Abstract

Aggressive cancer cells typically show a high rate of energy-consuming anabolic processes driving the synthesis of lipids, proteins, and DNA. Here, we took advantage of the ability of the cell-permeable nucleoside 5-aminoimidazole-4-carboxamide (AICA) riboside to increase the intracellular levels of AICA ribotide, an AMP analogue, mimicking a low energy status of the cell. Treatment of cancer cells with AICA riboside impeded lipogenesis, decreased protein translation, and blocked DNA synthesis. Cells treated with AICA riboside stopped proliferating and lost their invasive properties and their ability to form colonies. When administered *in vivo,* AICA riboside attenuated the growth of MDA-MB-231 tumors in nude mice. These findings point toward a central tie between energy, anabolism, and cancer and suggest that the cellular energy sensing machinery in cancer cells is an exploitable target for cancer prevention and/or therapy.

Introduction

Despite the marked genotypic heterogeneity resulting from the unique pathway traveled during carcinogenesis, cancer cells typically all strive to a common clinical behavior: relentless growth with progressive invasion of normal tissue. This paradox of common phenotypic behavior, despite a major genotypic diversity, has led to the appreciation of the existence of a limited set of exploitable hallmarks or phenotypic traits exhibited by virtually all aggressive cancers. One of these hallmarks is the high anabolic activity of cancer cells. Cancer cells typically overexpress lipogenic enzymes, including acetyl-CoA carboxylase and fatty acid synthase (1). They frequently show enhanced protein biosynthesis (2, 3) and are more active in synthesizing DNA. All these anabolic processes require energy and hence are expected to be regulated by the energy status of the cell, which is reflected in the cellular ATP/ AMP ratio. Under normal conditions, cellular AMP levels are very low, much lower than those of ATP. As a result, a small decrease in ATP levels results in a relatively large increase in AMP, rendering AMP a very sensitive indicator of the cellular energy status (4). Changes in cellular AMP levels allosterically regulate several metabolic enzymes, including glycogen phosphorylase and fructose-1,6-bisphosphatase (5-7), but above all are sensed by AMP-activated protein kinases (AMPK). AMPKs are a family of heterotrimeric serine/threonine kinases that on AMP binding are phosphorylated by upstream activating kinases (AMPK kinases). These include the tumor suppressor LKB1, which is inactivated in the Peutz-Jeghers syndrome, a familial colorectal polyp disorder in which patients are predisposed to early-onset cancers in many other tissues (8-12). AMPK kinase-induced phosphorylation of AMPKs at a conserved threonine residue in the activation loop of the catalytic α subunit (Thr172 of AMPKα1) activates all known AMPK homologues (13). Once activated, AMPKs phosphorylate several downstream targets. A prototypical target is acetyl-CoA carboxylase, the rate-determining enzyme in the synthesis of fatty acids (14, 15). Phosphorylation of acetyl-CoA carboxylase by AMPK in rat liver inactivates the enzyme by decreasing its V_{max} and its affinity for the allosteric activator citrate, thus shutting down this energy consuming pathway. Similarly, AMPK phosphorylates and inactivates 3-hydroxy-3-methylglutaryl CoA reductase (16), the rate-limiting enzyme in the synthesis of cholesterol and other isoprenoid compounds. Recent studies, mainly in liver and muscle, suggest that AMPK also affects protein synthesis both at the level of initiation of protein translation (phosphorylation of tuberous sclerosis component 2 and mammalian target of rapamycin) and at the level of elongation (eukaryotic elongation factor 2 kinase/ eukaryotic elongation factor 2; refs. 17-20).

The recent appreciation of tumor-associated anabolic processes (not only DNA synthesis but also the synthesis of proteins, fatty acids, and cholesterol) as individual targets for antineoplastic therapy (3, 21-25) has prompted us to explore the feasibility of targeting the energy sensing system in the battle against cancer. In this report, we have exploited the ability of exogenously added 5-aminoimidazole-4-carboxamide (AICA) riboside, a cell-

permeable nucleoside that on cell entry is converted to AICA ribotide (ZMP; ref. 26), to mimic the effects of AMP and have examined its potential to switch off cancer-related anabolism and to interfere with cancer cell biology.

Materials and Methods

Cell Culture.

MDA-MB-231 and LNCaP cells were obtained from the American Type Culture Collection (Manassas, VA). Cells were maintained at 37°C in a humidified incubator with a 5% CO_2/95% air atmosphere in RPMI 1640 supplemented with 10% FCS (Invitrogen, Carlsbad, CA).

Determination of ZMP Levels.

Cells (2×10^7) were treated with different concentrations of AICA riboside (Calbiochem, La Jolla, CA, or Toronto Research Chemicals, Toronto, Canada) for 2 hours. Cultures were washed twice with PBS, harvested, and centrifuged. Cell pellets were resuspended in 300 μL ice-cold 10% perchloric acid and incubated on ice for 15 minutes. After centrifugation at 12,000 × *g* for 5 minutes at 4°C, supernatants were neutralized with 5.0 mol/L potassium carbonate, recentrifuged, and stored at -80°C. Twenty microliters of each sample were diluted into 1 mL of 5 mmol/L ammonium acetate and loaded onto an Oasis MAX 3 cc/60 mg/30 μm cartridge (Waters). After washing with 2 mL of 5 mmol/L ammonium acetate and subsequently with 2 mL of 5% methanol, ZMP was eluted in 2 mL of 25% methanol with 2% formic acid. Eluates were dried and analyzed for ZMP content using tandem electrospray-mass spectrometry. Results were expressed as nanomoles per 10^7 cells.

Measurement of AMPK Activity.

Cells were cultured in 6-cm dishes and treated as indicated. Cultures were washed and lysed in homogenization buffer (50 mmol/L HEPES pH 7.4,50 mmol/L NaF, 5 mmol/L NaPPi, 1 mmol/L EDTA, 1 mmol/L EGTA, 10% glycerol, 1% Triton X-100, 1 mmol/L DTT, 1 mmol/L phenylmethylsulfonyl fluoride, 10 μg/mL aprotinin, 10 μg/mL leupeptin, and 5 μg/mL pepstatin A). Proteins were precipitated with 10% polyethylene glycol 6000. Pellets were redissolved and assayed for AMPK activity using SAMS peptide (200 μmol/L) in the presence of 200 μmol/L ATP, 1.6 μCi [γ-^{32}P]ATP, 5 mmol/L $MgCl_2$, and 200 μmol/L AMP. After incubation for 15 minutes at 30°C, the reaction mixture was spotted onto Whatman p81 paper. Papers were washed with 1% phosphoric acid and ^{32}P was counted using a scintillation counter.

Immunoblot Analysis.

Tissues or cells treated with different concentrations of AICA riboside and/or 5-iodotubercidin (Sigma, St. Louis, MO) were washed with PBS and lysed in a reducing NuPage sample loading buffer (Invitrogen). Protein concentrations were determined on aliquots after precipitation with trichloroacetic acid. Equal amounts of protein were separated on Tris-glycine (Fermentas, Hanover, MD) or NuPage (Invitrogen) gels and were blotted onto Hybond C+ membranes (Amersham). Membranes were blocked in a TBS solution with 5% nonfat dry milk and incubated with antibodies against AMPKα, phospho-Thrl72 AMPKα, eukaryotic elongation factor 2, phospho-Thr56 eukaryotic elongation factor 2, phospho-Ser79 acetyl-CoA carboxylase, cleaved poly(ADP-ribose) polymerase, and cytokeratin 18. All antibodies were from Cell Signaling Technologies (Beverly, MA) except anti-poly(ADP-ribose) polymerase-1 (BD Biosciences, San Jose, CA) and anti-cytokeratin 18 (Santa Cruz Biotechnology, Santa Cruz, CA). Horseradish peroxidase-conjugated secondary antibodies (DAKO, Carpinteria, CA) were used for detection of immuno-reactive proteins by chemiluminescence.

Incorporation of 2-[^{14}C]Acetate into Cellular Lipids.

Cells were plated in 6-cm dishes at a density of 0.5 to 1.5×10^6 cells per dish. The next day, medium was changed and cells were treated with AICA riboside and/ or with 5-iodotubercidin as indicated. After 1 or 24 hours of incubation, 2-[^{14}C]acetate (57 mCi/mmol; 2 μCi/dish; Amersham International, Aylesbury, United Kingdom) was added. Four hours later, cells were washed with PBS, scraped, and resuspended in 0.9 mL PBS. Lipids were extracted using the Bligh Dyer method as previously described (27, 28). Incorporation of ^{14}C into lipids was measured by scintillation counting. Measurements were done in triplicate and values were normalized for sample DNA content. Acetate incorporation into specific lipids was analyzed after separation of lipids by TLC (silica gel G plates, Merck, Darmstadt, Germany). Plates were developed in hexane-diethyl ether-acetic acid (70:30:1, v/v/v). ^{14}C incorporation into specific lipid classes was quantified using PhosphorImager screens

(Molecular Dynamics, Sunnyvale, CA) and normalized for sample DNA content.

Protein Synthesis Assay.

Cells cultured in 6-cm dishes were incubated with AICA riboside. After 4 to 20 hours, cultures were washed and incubated for 30 minutes with 0.5 μCi of [U-^{14}C]leucine in 2 mL of Krebs-Henseleit buffer (Sigma). Protein extracts were made in a homogenization solution (50 mmol/L HEPES pH 7.4,0.1% Triton X-100,50 mmol/L KCl,50 mmol/L KF, 5 mmol/L EDTA, 5 mmol/L EGTA, 1 mmol/L Na_3VO_4,0.1% 2-mercaptoethanol, 1 mmol/L potassium phosphate) and precipitated with trichloroacetic acid (10% final). Pellets were washed with 5% trichloroacetic acid and incorporation of ^{14}C into proteins was measured by scintillation counting.

Analysis of DNA Synthesis.

Cells were seeded on day 0 in 96-well plates at 5×10^3 cells per well. On day 2, cells were treated with AICA riboside in the absence or presence of 5-iodotubercidin as indicated. After 24 hours, cell proliferation was measured using the 5-bromo-2'-deoxy-uridine labeling and detection kit III (Roche, Basel, Switzerland).

Cell Counting.

Cells were plated in 6-cm dishes at a density of 4×10^5 cells/dish. The next day, cultures were treated with AICA riboside in the presence or absence of 10 nmol/L 5-iodotubercidin. At different time points after treatment, cells were trypsinized, stained with trypan blue, and counted.

Fluorescence-Activated Cell Sorting Analysis.

Cells were plated in 10-cm dishes at a density of 2×10^6 cells/dish. The next day, cells were treated with AICA riboside in the absence or presence of 10 nmol/L 5-iodotubercidin. At 48 or 72 hours after treatment, cells were trypsinized, fixed in 70% ice-cold ethanol, and washed twice with PBS ± 0.05% Tween 20 and incubated for 1 hour at room temperature with 0.05 mg/mL propidium iodide (Sigma) and 1 mg/iriL RNase A (Sigma). Cells were sorted and counted using a FACSort flow cytometer (BD Biosciences) using CellsQuest and Motfit software (BD Biosciences).

Hoechst Staining.

Cells were plated in 6-cm dishes at a density of 1×10^6 cells/dish. The next day, cultures were treated with AICA riboside in the presence or absence of 10 nmol/L 5-iodotubercidin. At 2 or 3 days after addition of these compounds, Hoechst dye 33342 (Sigma) was added to the culture medium in living cells. Changes in nuclear morphology were assessed by fluorescence microscopy.

Colony Formation Assay.

Cells were seeded at a density of 2×10^3 (or 5×10^3) cells per 6 cm dish. The next day, medium was changed and cells were treated with AICA riboside in the absence or presence of 5-iodotubercidin as indicated. After 3 days, medium was changed and treatment was repeated. Five to eight days after initial treatment, cultures were fixed with 4% formaldehyde in PBS and stained with a 0.5% crystal violet solution in 25% methanol. Colonies of more than 15 cells were counted.

Cell Migration and Matrix Invasion Test.

Cultures were treated with AICA riboside in the absence or presence of 5-iodotubercidin as indicated. After 20 hours of incubation, cells were trypsinized and reseeded at a density of 35×10^3 in the upper chamber of a modified Boyden two-chamber system [Corning Transwell, polycarbonate, pore size 8 μm (Corning, Inc., Acton, MA)]. Serum (10%) was added in the lower chamber as chemoattractant. For migration tests polycarbonate inserts were left untreated. For matrix invasion tests, polycarbonate inserts were coated with matrigel (BD Biosciences). After 4 hours (cell migration test) to 24 hours (matrix invasion test), remaining cells at the top surface of the membrane were removed using cotton swabs. Cells at the lower surface were fixed, stained with a 0.5% crystal violet solution in 25% methanol, and counted.

Tumor Xenograft Model.

MDA-MB-231 cells (2 x 10^6) were inoculated s.c. in 7-week-old female NMRI nu/nu mice at both flanks. Treatment was started when average tumor volumes reached 20 mm^3. Eight to ten mice were used per group. AICA riboside (Toronto Research Chemicals) was dissolved in 0.9% NaCl and administered i.p. (0.4 mg/g body weight). In one experiment animals were treated every other day. In another experiment, animals received AICA riboside daily. The control group received vehicle only (0.9% NaCl). Tumor size was measured once a week using calipers. Tumor volume was calculated using the formula $\pi / 6 \times A \times B^2$ (A = larger diameter of the tumor, B = smaller diameter of the tumor). After 4 weeks of treatment, animals were euthanized by cervical displacement. Tumors were resected 1 hour after the final treatment with AICA riboside or with vehicle and frozen in liquid nitrogen for analysis of ZMP, phospho-Thrl72 AMPKα, and AMPK. Experiments were done according to international regulations and were approved by the local Ethics Committee for Animal Experimentation of the Catholic University of Leuven.

Statistics.

Statistical analyses were done using one-way ANOVA with Dunnett's multiple comparison test Tumor volumes (AICA riboside-treated versus control) were compared using the Mann-Whitney test.

Results

Treatment of Cancer Cells with AICA Riboside Leads to Elevated ZMP Levels and Activates AMPK.

To assess the ability of exogenously added AICA riboside to be converted to ZMP in cancer cells, MDA-MB-231 cells and LNCaP cells (well-characterized models of breast cancer and prostate cancer, respectively) were incubated for 2 hours with increasing concentrations of AICA riboside and intracellular ZMP accumulation was measured. In untreated cells, ZMP was undetectable. A dose-dependent increase of ZMP levels was found after treatment with AICA riboside (Fig. 1*A*). To assess whether these changes in ZMP concentrations are sufficient to mimic cellular AMP responses, phosphorylation at Thr172 of the α catalytic subunit of prototypical AMPK family members (AMPK1 and AMPK2) was investigated by Western blot analysis with a phospho-AMPK-specific antiserum. Increased phosphorylation of AMPK was seen at AICA riboside concentrations that lead to a measurable increase of ZMP (0.250 mmol/L; Fig. 1*B).* Increased phosphorylation was detected as early as 15 minutes after addition of AICA riboside and (at least at the higher concentrations) was sustained for at least 24 hours (data not shown). Consistent with the increased phosphorylation of AMPK, treatment of the cells with AICA riboside resulted in increased AMPK activity as revealed by the elevation of *in vitro* phosphorylation of a synthetic SAMS peptide (Fig. 1C) and by the increased phosphorylation state of a well-known endogenous AMPK substrate, acetyl-CoA carboxylase (Fig. 1*D).* Similar results were obtained with the human prostate cancer cell line LNCaP (data not shown). These findings thus indicate that AICA riboside is taken up by cancer cells and is converted to ZMP, mimicking a low energy status of the cell.

AICA Riboside Inhibits Tumor-Associated Anabolism.

AICA riboside-induced activation of AMPK and subsequent phosphorylation of prototypical substrates such as acetyl-CoA carboxylase and 3-hydroxy-3-methylglutaryl CoA reductase in rat liver extracts have been linked with changes in total cellular lipogenesis (16). To investigate whether this is also the case in cancer cell lines, we treated MDA-MB-231 and LNCaP cells with increasing concentrations of AICA riboside and at different time points (1 and 24 hours) we added [C]acetate, which is taken up by the cells and is converted to [C]acetyl-CoA, the precursor of both fatty acid and cholesterol synthesis. After 4 hours of incubation, incorporation of [C] into extractable lipids was measured. Figure *2A* shows that treatment of MDA-MB-231 cells with AICA riboside resulted in a marked decrease of lipogenesis. Effects were seen at concentrations starting from 0.250 mmol/L, already 1 hour after addition of AICA riboside. At high concentrations of AICA riboside (2 mmol/L), lipogenesis was reduced to 8% of the control values. At the 24-hour time point, effects were even more pronounced (reduction to 2% of the control values), consistent with a sustained activation of AMPK and an additional down-regulation of lipogenic gene expression (data not shown) as previously reported in rat liver (ref. 29; Fig. *2A*). Similar observations were made in LNCaP cells (data not shown). Consistent with the involvement of ZMP in the antilipogenic effects of AICA riboside, 5-iodotubercidin, a potent inhibitor of adenosine kinase (the enzyme responsible for the intracellular conversion of AICA riboside to ZMP), counteracted the effects of AICA riboside (Fig. *2A).*

Previous studies have shown that the bulk of [C] label from [^{14}C]acetate in cancer cells is incorporated into

phospholipids, followed by triglycerides, cholesterol, and cholesteryl esters (22, 30). To examine the effect of AICA riboside treatment on the synthesis of these different lipid classes, lipid extracts were separated by TLC. Consistent with acetyl-CoA carboxylase, 3-hydroxy-3-methylglutaryl CoA reductase, and *sn* -glycerol-3-phosphate acyltransferase (14-16, 31) being substrates of AMPK, lipid classes affected by AICA riboside treatment included phospholipids, triglycerides, cholesterol, and cholesterol esters (Fig. *2B).* The synthesis of these lipids was almost equally down-regulated by AICA riboside and at higher concentrations of the nucleoside was almost completely blocked.

In order to assess whether AICA riboside also inhibits protein synthesis, we treated MDA-MB-231 cells with different concentrations of the nucleoside and labeled newly synthesized proteins with [C]leucine. At concentrations starting from 0.5 mmol/L, AICA riboside inhibited protein translation, with a maximal reduction to 20% to 40% (depending on the experiment) of the control levels (Fig. 3*A*). 5-Iodotubercidin largely counteracted the effects of AICA riboside. Effects on protein synthesis were associated with increased phosphorylation of eukaryotic elongation factor 2 at an AMPK target site (Fig. 35).

Another key anabolic process in rapidly dividing cancer cells is the synthesis of DNA. To investigate whether this process is also affected by AICA riboside, cells were pretreated with AICA riboside and the incorporation of BrdUrd was assessed. Treatment of MDA-MB-231 cells with AICA riboside caused a potent and dose-dependent reduction of BrdUrd incorporation with a maximal reduction to 15% of the control levels (Fig. 3C). 5-Iodotubercidin displayed some inhibiting effects on its own, yet largely reversed the effects of AICA riboside.

Figure 1: *AICA riboside increases ZMP levels and activates AMPK in MDA-MB-231 cancer cells. A, ZMP measurement. Cells were treated with different concentrations of AICA riboside for 2 hours and ZMP levels were measured using electrospray-mass spectrometry. Columns, means of triplicate measurements; bars, SE. B, immonoblot analysis of phospho-Thr172 AMPKα. Cells were treated with different concentrations of AICA riboside for 3 hours. Equal amounts of proteins were subjected to immunoblot analysis with an antiserum against phospho-Thr172 AMPKα (pAMPK) or AMPK irrespective of its phosphorylation state (AMPK). Results are representative of four independent experiments. C, AMPK activity test. After 2 hours of incubation with the indicated concentration of AICA riboside, cell extracts were assayed for their ability to phosphorylate a synthetic SAMS peptide in vitro in the presence of [γ-^{32}P]ATP. Values were corrected for differences in protein concentration; columns, means of triplicate measurements of two experiments done; bars, SE. *, P < 0.01 versus untreated cells (0 mmol/L AICA riboside). D, AICA riboside-induced phosphorylation of acetyl-CoA carboxylase in intact MDA-MB-231 cells. Cells were treated for 3 hours with different concentrations of AICA riboside. Equal amounts of proteins were subjected to Western blot analysis with an antiserum against phospho-Ser79 acetyl-CoA carboxylase (pACC). Equal loading of proteins was confirmed by immunoblotting for cytokeratin 18 (CK18). Results are representative of four independent experiments.*

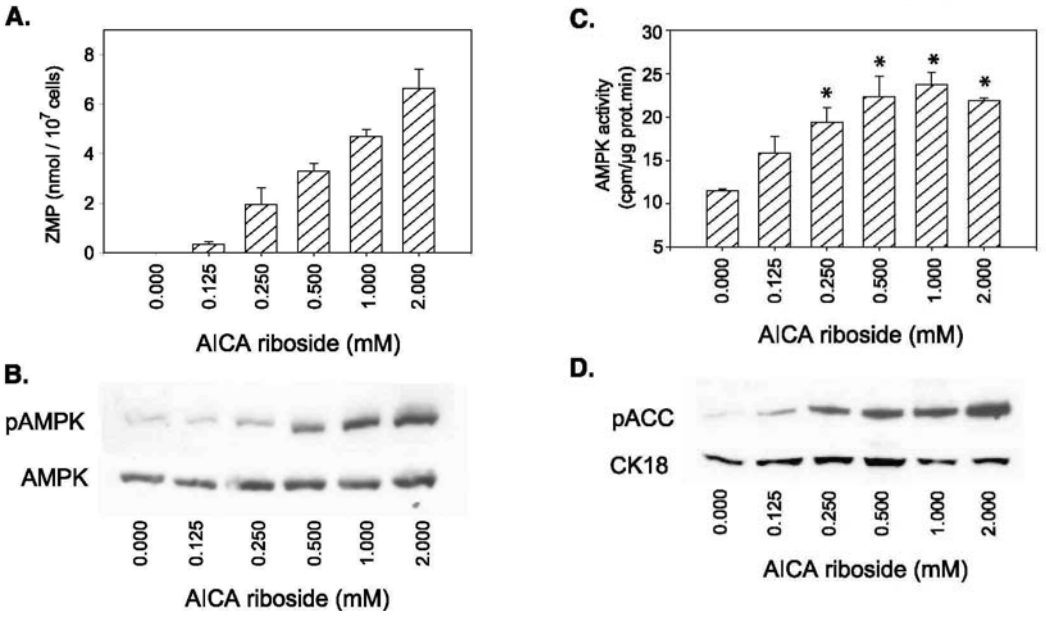

Published in: Cancer Research (2005), vol.65, iss.6, pp.2441-8
Status: Postprint (Author's version)

Figure 2: *AICA riboside inhibits lipogenesis in cancer cells. A, MDA-MB-231 cells were treated with different concentrations of AICA riboside in the absence (left) or in the presence of 10 nmol/L 5-iodotubercidin (right). At the indicated time after treatment, [^{14}C]acetate was added. Four hours later, lipids were extracted. ^{14}C incorporation in lipids was measured. Values were corrected for differences in DNA content of the cultures and expressed relative to the values of the untreated cells. A 0.000, no AICA riboside; A 1.000, 1 mmol/L AICA riboside. Columns, means of three values; bars, SE. IT, 5-iodotubercidin. B, lipid extracts from the 24-hour time point of A were separated by TLC. ^{14}C incorporation into specific classes of lipids was measured using Phosphorlmager screens and expressed as densitometric units. Plipids, phospholipids; Chol, cholesterol; TAG, triacylglycerol; CE, cholesteryl esters.*

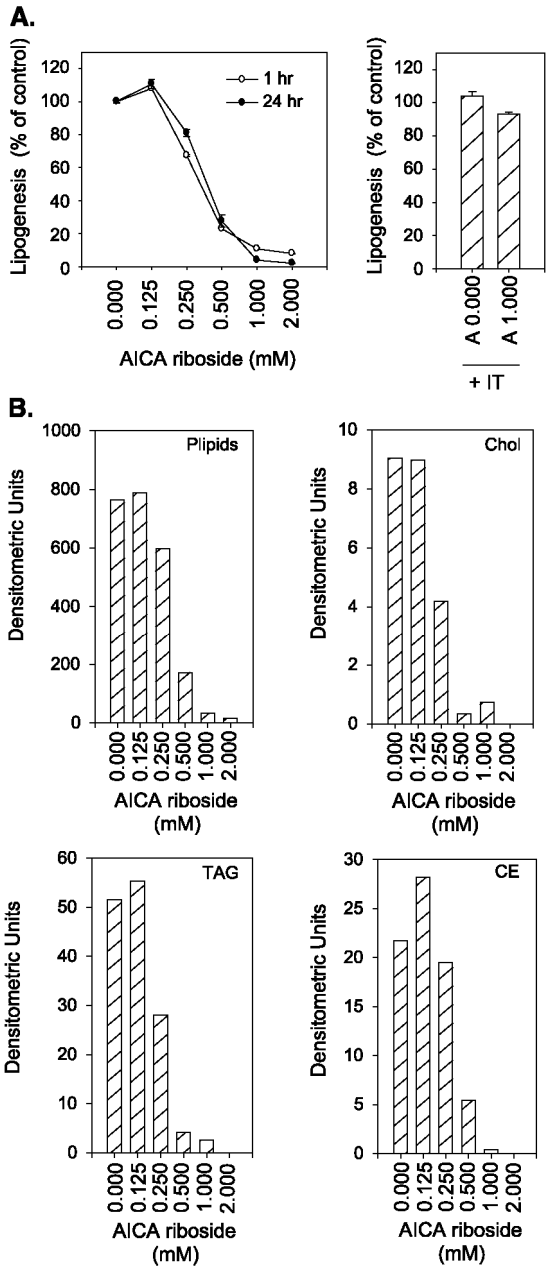

Effect of AICA Riboside on Tumor-Associated Cell Functions: Cell Proliferation, Cell Survival, Colony Formation, Migration, and Matrix Invasion.

Next we examined to what extent AICA riboside-induced inhibition of tumor-associated anabolism affects downstream tumor-associated cell functions such as cell proliferation, cell survival, colony formation, migration, and matrix invasion. To assess the effect on cell proliferation and cell survival, we treated MDA-MB-231 cells with AICA riboside and at different time points after drug addition counted the number of living cells by trypan blue exclusion tests. Whereas the number of cells in control conditions increased exponentially in function of the time of incubation, AICA riboside caused a complete stagnation of the number of living cells (Fig. *4A).* Significant effects were seen 2 days after addition of AICA riboside. Analysis of the cell cycle distribution by

fluorescence-activated cell sorting revealed that AICA riboside induced an accumulation of cells in the S-phase of the cell cycle, signifying an impediment of S-phase progression due to the low anabolic activity (Fig. *4B).* 5-Iodotubercidin largely prevented the AICA riboside-induced changes in cell cycle distribution (Fig. *4B).* At 3 days after treatment, an increase in the number of dead cells was noticed, particularly at high concentrations of AICA riboside. At 1 mmol/L, AICA riboside induced cell death in 30% of the cells (Fig. *4A).* At 2 mmol/L this percentage increased to 50% (data not shown). In support of the involvement of apoptosis, AICA riboside induced chromatin condensation and nuclear fragmentation and led to caspase-dependent cleavage of poly(ADP-ribose) polymerase (data not shown).

The inhibition of cell proliferation and the partial induction of apoptosis at high concentrations of AICA riboside (>1 mmol/L) were reflected also in the ability of cancer cells to form colonies. MDA-MB-231 cells were plated at a low density and treated with different concentrations of AICA riboside. Administration of AICA riboside once every 3 days was sufficient to cause a dose-dependent decrease both in the size and in the number of colonies. At 1 mmol/L, AICA riboside caused a 5-fold reduction of the number of colonies (Fig. 4C). At 2 mmol/L nearly no colonies were observed after 10 days of treatment. 5-Iodotubercidin largely reversed the effect of AICA riboside on colony formation.

Next we examined the effect of AICA riboside on the invasive behavior of MDA-MB-231 cells. MDA-MB-231 represents an aggressive cell line that rapidly migrates toward chemoattractants present in serum and efficiently migrates through a reconstituted extracellular matrix. Cells were pretreated with different concentrations of AICA riboside, and cell migration and invasiveness were assessed using a modified two-well Boyden chamber without or with Matrigel coating, respectively. Treatment of cancer cells with AICA riboside caused a strong dose-dependent decrease in the migration of cells (Fig. 5*A*). Also the number of cells that migrated through the Matrigel matrix was markedly reduced (Fig. *5B).* As the decrease in cell migration and invasiveness was observed within 24 hours after addition of AICA riboside and already at low concentrations, changes in cell number or induction of apoptosis cannot account for the observed effects. Cotreatment with 5-iodotubercidin restored migration and invasiveness. Together, these data show that mimicry of a low energy status in cancer cells by AICA riboside-induced ZMP accumulation leads cancer cells into a stage of anergy, blocking all cancer cell-associated processes, including cell proliferation, colony formation, migration, and matrix invasion.

Figure 3: *Effect of AICA riboside on protein translation and DNA synthesis. A, ^{14}C-leucine incorporation test. MDA-MB-231 cells were treated for 20 hours with different concentrations of AICA riboside in the absence or presence of 10 nmol/L 5-iodotubercidin. After incubation with 0.5 μCi [U-^{14}C]leucine for 30 minutes, proteins were precipitated with trichloroacetic acid. ^{14}C incorporation into proteins was measured by scintillation counting. *, P < 0.05 (n = 3) versus untreated cells (0 mmol/L AICA riboside). B, immunoblot analysis of phospho-eukaryotic elongation factor 2. Cells were treated with AICA riboside as indicated. After 4 hours of incubation, total protein extracts were made. Equal amounts of proteins were subjected to immunoblot analysis with an antiserum against phospho-Thr56 eukaryotic elongation factor 2 (peEF2) or against total eukaryotic elongation factor 2 (eEF2) irrespective of the phosphorylation status. Results are representative of two independent experiments. C, BrdUrd incorporation test. MDA-MB-231 cells were seeded in 96-well plates at 5 × 10^3 cells/well. Two days later, cells were treated with AICA riboside in the absence or presence of 10 nmol/L 5-iodotubercidin. After 24 hours, BrdUrd was added and incorporation into DNA was measured. Points, means of quadruplicates from one experiment representative of two experiments done; bars, SE. *, P < 0.01 versus 0 mmol/L AICA riboside.*

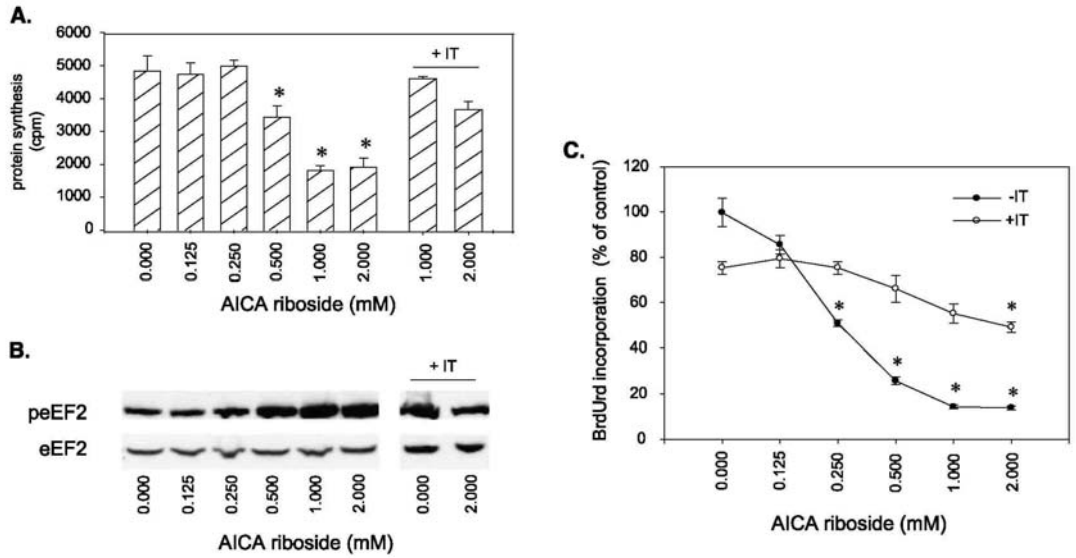

Published in: Cancer Research (2005), vol.65, iss.6, pp.2441-8
Status: Postprint (Author's version)

Figure 4: *Effect of AICA riboside on cell proliferation and colony formation. A, cell counting. MDA-MB-231 cells were plated at a density of 4 × 10^5 cells/6 cm dish. The next day cultures were treated with different concentrations AICA riboside. At the indicated time points, cells were trypsinized and stained with trypan blue. Trypan blue-negative (Living) cells and trypan blue-positive (Dead) cells were counted. Points, means of triplicates from one experiment representative of two experiments done; bars, ± SE. B, fluorescence-activated cell sorting analysis. Cells were cultured for 2 days in the absence (A 0.000) or in the presence (A 1.000) of 1 mmol/L AICA riboside with 10 nmol/L 5-iodotubercidin (+/T) or without, and subjected to fluorescence-activated cell sorting analysis. Shown are the mean percentages of cells in different phases of the cell cycle ± SE of four measurements of two independent experiments. C, colony formation. MDA-MB-231 cells were seeded at a density of 3 × 10^5 cells per 6-cm dish. The next day cultures were treated with different concentrations of AICA riboside in the absence or in the presence of 5-iodotubercidin. Three days later, medium was changed and treatment was repeated. Eight days after initial treatment, cultures were fixed with 4% formaldehyde in PBS and stained with a 0.5% crystal violet solution in 25% methanol. Colonies of more than 15 cells were counted. Columns, means of measurements in triplicate; bars, SE. Shown is a representative experiment of the three experiments done. *, P < 0.01 versus untreated cultures (0 mmol/L AICA riboside).*

A.

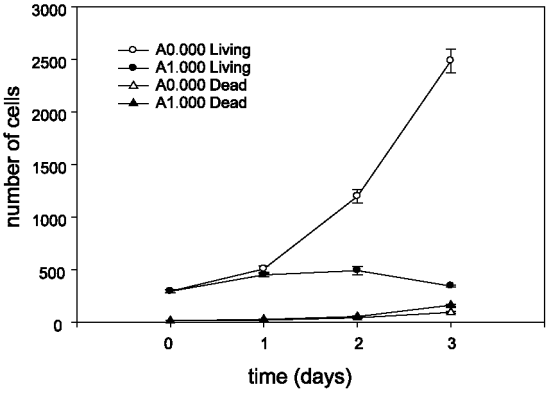

B.

	G0-G1	S	G2-M
A 0.000	72.0 +/- 1.4	18.1 +/- 0.7	9.9 +/- 0.7
A 1.000	49.0 +/- 0.6	43.5 +/- 1.5	7.5 +/- 1.5
A 0.000 + IT	70.3 +/- 0.1	18.8 +/- 0.6	10.9 +/- 1.3
A 1.000 + IT	69.4 +/- 0.9	19.7 +/- 0.9	10.9 +/- 0.8

C.

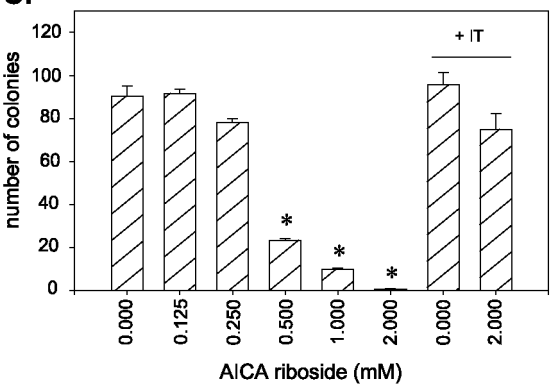

AICA Riboside Attenuates the Growth of Cancer Cells in Nude Mice In vivo.

In a final step of this study, we explored to what extent AICA riboside affects the growth of cancer cells in an *in vivo* situation. Therefore we inoculated immunodeficient nude mice s.c. with MDA-MB-231 cells. When the tumors reached an average volume of 20 mm^3, animals were treated i.p. with 0.4 mg AICA riboside/g body weight every other day (Fig. 6). Measurements of the changes in tumor volume in function of time revealed that AICA riboside treatment caused a significant reduction in tumor growth in comparison with the vehicle-treated controls. In 3 of 17 inoculations in the AICA riboside-treated group no significant tumor growth was observed (versus 0 of 20 in the control group). Similar results were obtained when AICA riboside was administered daily (data not shown). Suppression of tumor growth was accompanied by increased levels of ZMP in tumors of AICA riboside-treated animals (1.28 ± 0.39 nmol/mg tissue in the AICA riboside-treated group versus 0.034 ± 0.001

nmol/mg tissue in the control group) and by activation of AMPK (data not shown). Body weight of the animals was not affected.

Figure 5: *Effect of AICA riboside on cell migration and on matrix invasion. A, cell migration test. MDA-MB-231 cells were treated with different concentrations of AICA riboside in the absence or in the presence of 5-iodotubercidin (+/T). Twenty hours later, cells were trypsinized and reseeded in the upper chamber of a modified Boyden two-chamber system, with 10% serum in the lower well as chemoattractant. After 4 hours, cells at the lower surface were counted. B, matrix invasion test. Cells were treated as in A and seeded in polycarbonate inserts coated with matrigel. Twenty-four hours later, cells at the lower surface were counted. Columns, means of measurements in triplicate; bars, SE. Shown are representative experiments of two experiments done. *, P < 0.01 versus untreated cells (0 mmol/L AICA riboside).*

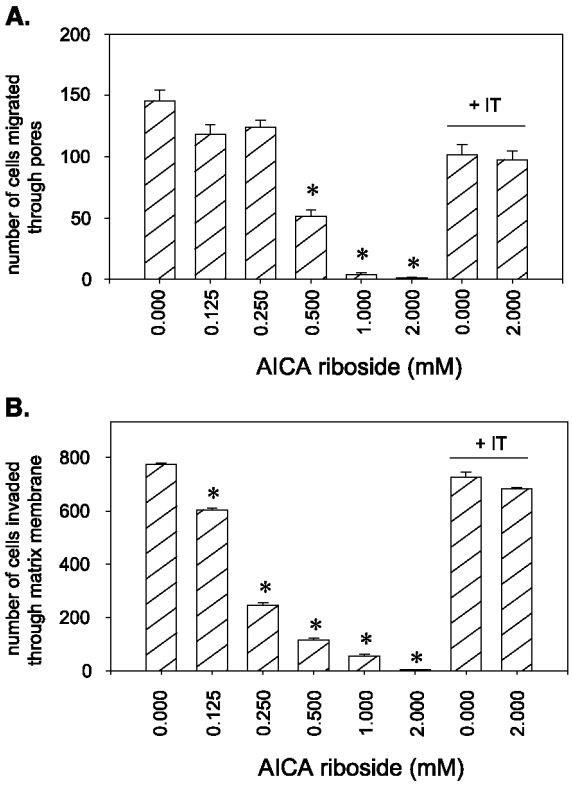

Discussion

Given that aggressive cancer cells have a high energy-demanding anabolic activity and that anabolism is intrinsically regulated by the cellular energy supply, we explored whether interference with the energy sensing machinery of cancer cells halts the anabolic phenotype and affects cancer cell biology. In the present report, we mimicked a cellular low energy status in MDA-MB-231 and LNCaP cancer cell lines by treating them with the cell-permeable nucleoside AICA riboside. We found that AICA riboside is taken up by the cells and is efficiently converted to ZMP, a potent mimetic of the cellular low energy indicator AMP. In support of the successful mimicry of a low cellular energy status, AMPK was activated. This activation occurred despite the absence of LKB1 in MDA-MB-231 cells (32), suggesting that other AMPK kinases may be involved. Importantly, AICA riboside largely inhibited major tumor-associated anabolic processes (the synthesis of lipids, proteins, and DNA), impeded cell proliferation, blocked the formation of colonies, inhibited cell migration and matrix invasion, and at high concentrations (>l mmol/L) induced apoptosis. Cotreatment with 5-iodotubercidin, which prevents the conversion of AICA riboside to ZMP, counteracted all these effects and largely restored the malignant phenotype. As evidenced by the increased phosphorylation of acetyl-CoA carboxylase and eukaryotic elongation factor 2, lipogenesis and protein synthesis were affected directly by ZMP-induced AMPK activation. Tumor-related cell functions such as proliferation, survival, migration, and invasiveness were probably affected indirectly as a consequence of the observed changes in the anabolism. In fact, down-regulation of lipogenesis by selective knockdown of fatty acid synthase has been shown to exert effects on cell proliferation and survival (22). Similarly, inhibition of 3-hydroxy-3-methylglutaryl CoA reductase by statins, through inhibition of cholesterol synthesis and/or production of prenyl groups, affects cell proliferation, induces apoptosis, and inhibits motility (for review see refs. 23 and 33). As AICA riboside severely blocks all these metabolic pathways simultaneously, AICA riboside-induced inhibition of anabolism is thought to play a major role in the observed

attenuation of malignancy-related functions, thus providing evidence for a direct link between energy status, tumor-associated anabolism, and malignant phenotype. The existence of such a link is of particular interest in view of the high energy intake in western countries and of existing literature showing a correlation between energy restriction and decreased cancer incidence (34, 35). The ability of AICA riboside to attenuate the growth of xenografted MDA-MB-231 tumors in nude mice *in vivo* suggests that the energy sensing machinery may also be a novel target for cancer prevention and/or for cancer growth retardation. Our observation that AICA riboside led to increased ZMP levels and activation of AMPK in tumors suggests that at least part of the observed effects are exerted directly in the tumor cells as in the *in vitro* situation. However, consistent with previous *in vivo* studies using this compound (36), AICA riboside also activated AMPK in a number of normal tissues (data not shown). These effects may indirectly contribute to the observed antitumoral effects of AICA riboside. Interesting in this respect is the finding that chronic whole body administration of AICA riboside in laboratory animals largely mimics the effects of long-term exercise, which also has been shown to increase AMPK activity (37-39) and has been linked to a reduced risk of cancer both in animal models and in humans (40, 41). It is unlikely, however, that AICA riboside per se will ultimately be useful as an antineoplastic agent. Although AICA riboside is well tolerated (42), the clinical use of AICA riboside is limited by the large amount of drug that is needed to exert effects. The exploitation of the energy sensing machinery as a target for cancer prevention and/or tumor growth retardation may therefore have to await the development of techniques to enhance the efficacy of AICA riboside or of more potent alternative activators of AMPK. The fact that the expression of individual components of the energy sensing machinery (e.g., LKB1) may be altered in cancer cells versus normal cells, together with the evidence that these changes may provide a therapeutic window in which tumor cells may be particularly sensitive to AMP analogues (12), urges to delineate to what extent different members of the AMPK kinase and the AMPK family are involved in the antimetabolic and antitumorigenic effects of AMP analogues. A better insight into these processes will facilitate the design of novel treatment regimens that more selectively and more effectively target the link between the energy sensing system and the anabolic pathways in cancer cells.

Figure 6: *AICA riboside retards the growth of MDA-MB-231 tumor xenografts in nude mice. MDA-MB-231 cells (2 × 10^6) were inoculated s.c. in nude mice. When the tumors reached an average volume of 20 mm^3, mice were treated i.p. with 0.4 mg AICA riboside/g body weight every other day. The control group received vehicle only (0.9% NaCI). Tumor volumes were measured once a week. Points, means of 20 tumors in the control group and of 17 tumors in the AICA riboside-treated group; bars, SE. *, P < 0.01 versus vehicle-treated controls.*

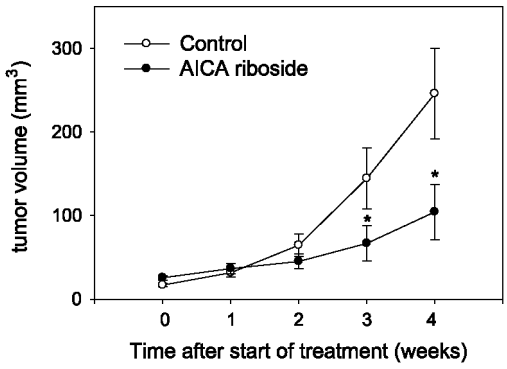

Acknowledgments

Grant support: Cancer Research grant from Fortis Bank Insurance, a grant from a Concerted Research Action (Research Fund, Catholic University of Leuven), research grants from the Fund for Scientific Research-Flanders (Belgium), and a grant from the Interuniversity Poles of Attraction Programme-Belgian State, Prime Minister's Office, Federal Office for Scientific, Technical and Cultural Affairs. T. Van de Sande and L. Timmermans are research assistants and K. Brusselmans is a postdoctoral fellow of the Fund for Scientific Research-Flanders (Belgium).

The costs of publication of this article were defrayed in part by the payment of page charges. This article must therefore be hereby marked *advertisement* in accordance with 18 U.S.C. Section 1734 solely to indicate this fact.

References

1. Kuhajda FP. Fatty acid synthase and human cancer: new perspectives on its role in tumor biology. Nutrition 2000;16:202-8.

2. Pandolfi PP. Aberrant mRNA translation in cancer pathogenesis: an old concept revisited comes finally of age. Oncogene 2004;23:3134-7.

3. Abdulov S, Li S, Mochalek V, et al. Activation of translation complex eIF4F is essential for the genesis and maintenance of the malignant phenotype in human mammary epithelial cells. Cancer Cell 2004;5:553-63.

4. Carling D. The AMP-activated protein kinase cascade: a unifying system for energy control. Trends Biochem Sci 2004;29:18-24.

5. Barford D, Johnson LN. The allosteric transition of glycogen phosphorylase. Nature 1989;340:609-16.

6. Claus TH, El-Maghrabi MR, Regen DM, et al. The role of fructose 2,6-bisphosphate in the regulation of carbohydrate metabolism. Curr Top Cell Regul 1984; 23:57-86.

7. Rakus D, Tillmann H, Wysocki R, Ulaszewski S, Eschrich K, Dzugaj A. Different sensitivities of mutants and chimeric forms of human muscle and liver fructose-1,6-bisphosphatases towards AMP. Biol Chem 2003;384:51-8.

8. Boudeau J, Sapkota G, Alessi DR. LKB1, a protein kinase regulating cell proliferation and polarity. FEBS Lett 2003;546:159-65.

9. Hawley SA, Boudeau J, Reid JL, et al. Complexes between the LKB1 tumor suppressor, STRADα/β and M025 α/β are upstream kinases in the AMP-activated protein kinase cascade. J Biol 2003;2:28.1-28.16.

10. Woods A, Johnstone SR, Dickerson K, et al. LKB1 is the upstream kinase in the AMP-activated protein kinase cascade. Curr Biol 2003;13:2004-8.

11. Lizcano JM, Goransson O, Toth R, et al. LKB1 is a master kinase that activates 13 kinases of the AMPK subfamily, including MARK/PAR-1. EMBO J 2004;23: 833-43.

12. Shaw RJ, Kosmatka M, Bardeesy N, et al. The tumor suppressor LKBl kinase directly activates AMP-activated kinase and regulates apoptosis in response to energy stress. Proc Natl Acad Sci U S A 2004;101:3329-35.

13. Hardie DG. Minireview: the AMP-activated protein kinase cascade: the key sensor of cellular energy status. Endocrinology 2003;144:5179-83.

14. Carling D, Zammit VA, Hardie DG. A common bicyclic protein kinase cascade inactivates the regulatory enzymes of fatty acid and cholesterol biosynthesis. FEBS Lett 1987;223:217-22.

15. Munday MR, Cambell DG, Carling D, Hardie DG. Identification by amino acid sequencing of three major regulatory phosphorylation sites on rat acetyl-CoA carboxylase. Eur J Biochem 1988;175:331-8.

16. Clarke PR, Hardie DG. Regulation of HMG-CoA reductase: identification of the site phosphorylated by the AMP-activated protein kinase *in vitro* and in intact rat liver. EMBO J 1990;9:2439-46.

17. Bolster DR, Crozier SJ, Kimball SR, Jefferson LS. AMP-activated protein kinase suppresses protein synthesis in rat skeletal muscle through down-regulated mammalian target of rapamycin (mTOR signaling). J Biol Chem 2002;277:23977-80.

18. Horman S, Browne G, Krause U, et al. Activation of AMP-activated protein kinase leads to the phosphorylation of elongation factor 2 and an inhibition of protein synthesis. Curr Biol 2002;12:1419-23.

19. Browne GJ, Finn SG, Proud CG. Stimulation of the AMP-activated protein kinase leads to activation of eukaryotic elongation factor 2 kinase and to its phosphorylation at a novel site, serine 398. Oncogene 2004;23:3151-71.

20. Inoki K, Zhu T, Guan KL. TSC2 mediates cellular energy response to control cell growth and survival. Cell 2003;115:577-90.

21. Kuhajda FP, Jenner K, Wood FD, et al. Fatty acid synthesis: a potential selective target for antineoplastic therapy. Proc Natl Acad Sci U S A 1994;91:6379-83.

22. De Schrijver E, Brusselmans K, Heyns W, Verhoeven G, Swinnen JV. RNA interference-mediated silencing of the fatty acid synthase gene attenuates growth and induces morphological changes and apoptosis in LNCaP prostate cancer cells. Cancer Res 2003;63:3799-804.

23. Jakobisiak M, Golab J. Potential antitumor effects of statins (Review). Int J Oncol 2003;23:1055-69.

24. Fingar DC, Blenis J. Target of rapamycin (TOR): an integrator of nutrient and growth factor signals and coordinator of cell growth and cell cycle progression. Oncogene 2004;23:3151-71.

25. De Benedetti A, Graff JR. eIF-4E expression and its role in malignancies and metastases. Oncogene 2004; 23:189-99.

26. Corton JM, Gillespie JG, Hawley SA, Hardie DG. 5-Aminoimidazole-4-carboxamide ribonucleoside. A specific method for activating AMP-activated protein kinase in intact cells? Eur J Biochem 1995;229:558-65.

27. Swinnen JV, Van Veldhoven PP, Esquenet M, Heyns W, Verhoeven G. Androgens markedly stimulate the accumulation of neutral lipids in the human prostatic adenocarcinoma cell line LNCaP. Endocrinology 1996; 137:4468-74.

28. Swinnen JV Esquenet M, Goossens K, Heyns W, Verhoeven G. Androgens stimulate fatty acid synthase in the human prostate cancer cell line LNCaP. Cancer Res 1997;57:1086-90.

29. Ferré P, Azzout-Marniche D, Foufelle F. AMP-activated protein kinase and hepatic genes involved in glucose metabolism. Biochem Soc Trans 2003;31:220-3.

30. Swinnen JV Van Veldhoven PP, Timmermans L, et al. Fatty acid synthase drives the synthesis of phospholipids partitioning into detergent-resistant membrane microdomains. Biochem Biophys Res Commun 2003;302:898-903.

31. Muoio DM, Seefeld K, Witters LA, Coleman RA AMP-activated kinase reciprocally regulates triacylglycerol synthesis and fatty acid oxidation in liver and muscle: evidence that *sn*-glycerol-3-phosphate acyltransferase is a novel target. Biochem J 1999;338:783-91.

32. Shen Z, Wen XF, Lan F, Shen ZZ, Shao ZM. The tumor suppressor gene LKB1 is associated with prognosis in human breast carcinoma. Clin Cancer Res 2002;8:2085-90.

33. Wong WW, Dimitroulakos J, Minden MD, Penn LZ. HMG-CoA reductase inhibitors and the malignant cell: the statin family of drugs as triggers of tumor-specific apoptosis. Leukemia 2002;16:509-19.

34. Kritchevsky D. Caloric restriction and cancer. J Nutr Sci Vitaminol (Tokyo) 2001;47:13-9.

35. Dirx MJM, Zeegers MPA, Dagnelie PC, Van den Bogaard T, Van den Brandt PA. Energy restriction and the risk of spontaneous mammary tumors in mice: a meta-analysis. Int J Cancer 2003;106:755-70.

36. Buhl ES, Jessen N, Pold R, et al. Long-term AICAR administration reduces metabolic disturbances and lowers blood pressure in rats displaying features of the insulin resistance syndrome. Diabetes 2002;51: 2199-206.

37. Carlson CL, Winder WW. Liver AMP-activated protein kinase and acetyl-CoA carboxylase during and after exercise. J Appl Physiol 1999;86:669-74.

38. Holmes BF, Kurth-Kraczek EJ, Winder WW. Chronic activation of 5' AMP-activated protein kinase increases GLUT-4, hexokinase, and glycogen in muscle. J Appl Physiol 1999;87:1990-5.

39. Winder WW, Holmes BF, Rubinck DS, Jensen EB, Chen M, Holloszy JO. Activation of AMP-activated protein kinase increases mitochondrial enzymes in skeletal muscle. J Appl Physiol 2000;88:2219-26.

40. Thune I, Brenn T, Lund E, Gaard M. Physical activity and the risk of breast cancer. New Engl J Med 1997;336:1269-75.

41. Friedenreich CM, Orenstein MR. Physical activity and cancer prevention: etiologic evidence and biological mechanisms. J Nutr 2002;132:3456-64S.

42. Dixon R, Gourzis J, McDermott D, Fujitaki J, Dewland P, Gruber H. AICA riboside: safety, tolerance, and pharmacokinetics of a novel adenosine-regulating agent. J Clin Pharmacol 1991;31:342-7.